# Influence of solvent treatment with fluoro compounds on the properties of poly(3,4-ethylenedioxythiophene): poly(styrene sulfonate) polymer as a hole transport layer in polymer solar cells

Palanisamy Kumar
Abhirami Kumar
Paik-Kyun Shin
Shizuyasu Ochiai

# Influence of solvent treatment with fluoro compounds on the properties of poly(3,4-ethylenedioxythiophene): poly(styrene sulfonate) polymer as a hole transport layer in polymer solar cells

**Palanisamy Kumar,[a] Abhirami Kumar,[a] Paik-Kyun Shin,[b] and Shizuyasu Ochiai[a],***

[a]Aichi Institute of Technology, Department of Electrical Engineering, Toyota 470-0392, Japan
[b]Inha University, School of Electrical Engineering, 253 Yonghyun-gong, Incheon 402-751, Republic of Korea

**Abstract.** We prepared high conducting poly(3,4-ethylenedioxythiophene):poly(styrene sulfonate) (PEDOT:PSS) by solvent additives for using as a hole transport layer (HTL) in polymer solar cells (PSCs). PEDOT:PSS films treated with fluoro compounds of hexafluoroacetone (HFA) and hexafluoroisoproponal (HFIPA) with various concentrations show a significant enhancement in electrical conductivity without compromising optical transparency. The conductivity increased from 0.2 to 1053 and 746 S/cm after 4 vol. % HFA and 6 vol. % HFIPA treatments, respectively. The high performance of the PEDOT:PSS layer is attributed to preferential phase segregation of PEDOT:PSS with HFA and HFIPA solvent mixture treatment methods. The improved performance of PSC was dependent on the structure of organic solvents and the concentration of fluoro compounds in PEDOT:PSS solution. Using these optimized layers, conjugated PSCs with a poly[[9-(1-octylnonyl)-9H-carbazole-2,7-diyl]-2,5-thiophenediyl-2,1,3-benzothiadiazole-4,7-diyl-2,5 thiophenediyl] polymer:[6,6]-phenyl-C71-butyric acid methyl esters (PCDTBT:PC$_{71}$BM) bulk heterojunction have been produced. The high power conversion efficiency (PCE) of 4.10% and 3.98% were observed for PEDOT:PSS films treated with 4 vol. % HFA and 6 vol. % HFIPA treatments, respectively. The obtained results show that PEDOT:PSS optimized with HFA and HFIPA organic solvents can be a very promising candidate for transparent anode buffer layer in the low cost organic solar cell devices. © *The Authors. Published by SPIE under a Creative Commons Attribution 3.0 Unported License. Distribution or reproduction of this work in whole or in part requires full attribution of the original publication, including its DOI.* [DOI: 10.1117/1.JPE.4.043097]

## 1 Introduction

The rise in global energy consumption as a result of increase in the population of the world and the subsequent decrease in fossil fuel resources is a serious matter of concern. Renewable energy is considered to be one of the alternative solutions to reduce environmental issues such as global warming and climate change. Harvesting energy directly from solar radiation through photovoltaic technology is a well-established strategy of future global energy production.[1] The current research community is extensively involved in developing new materials for green and clean energy applications. Among them, polymer solar cell (PSC) is one of the most important applications. The striking achievements in photoconducting polymers have opened a new pathway, and researchers have found that organic semiconducting polymers play an important role in

efficient solar energy conversion.[2] PSCs based on conjugated polymer materials have been the focus of intense research over the past 15 years through the development of bulk heterojunction (BHJ) architectures comprising a donor-acceptor (D-A) systems, where efficient exciton dissociation takes place. Continuous improvements of the solar cell structure and the power conversion efficiency (PCE) have resulted from the developments of low bandgap polymer materials, novel approaches to control the active layer morphology, and various combinations of D-A materials.[3,4]

PSCs are the best alternative to their inorganic counterparts because of their attractive features, which include light weight, high flexibility, roll-to-roll process, ease of large-area fabrication, and potential for low-cost solution processing.[5,6] These advantages are due to the preparation of solar cells using solution processes at room temperature such as spin or spray coating. The research activities and reports on PSC-based devices have been increased during the last two decades. Researchers have adopted many ways to achieve high PCE in PSCs and to cover a large area at low cost.[7] Among the various polymers used, conjugated low bandgap polymer-based active layers yield high PCE of 5–9%[8–11] while >10% are needed for commercial viability.[12] The performance of PSCs has been improved using new materials, new structures, and new techniques in devices.[13,14] Recently, interest has been focused on fabricating solar cells utilizing low energy-gap polymers as the light absorbing and electron donating material combined with an electron accepting fullerene derivative. One such low energy-gap polymer is poly [N-9-heptadeca-nyl-2,7-carbazole-alt-5,5(4,7-di-2-thienyl-2,1,3-benzo-thiadiazole)] (PCDTBT).[15–19] The extended red absorption of such materials can lead to improved performance by harvesting a greater fraction of the sun's radiation.

To achieve the optimal PCE of a solar cell, the use of an additional interface layer is essential. The interface layer modification on BHJ active layer/electrodes has been comprehensively carried out for the improvement of charge injection or collection, especially those due to mismatched energy levels between polymer materials and metal electrodes.[20–22] In order to enhance the PCE, several buffer layers have been reported to modify the interface between the active layer and metal electrodes. Many materials such as poly(3,4-ethylenedioxythiophene):poly(styrene sulfonate) (PEDOT:PSS), molybdenum trioxide ($MoO_3$), vanadium pentoxide ($V_2O_5$), nickel oxide ($NiO_2$), and tungsten oxide ($WO_3$) have been used as hole transport buffer layers,[23–26] and titania ($TiO_x$), lithium fluoride (LiF), cesium carbonate ($CsCO_3$), and zinc oxide (ZnO) have been reported for electron extraction layers[27–30] to improve the device performance. Among the several anode buffer layer materials, PEDOT:PSS is widely used as anode buffer layer due to its high transparency in the visible region, high thermal stability, and mechanical flexibility. PEDOT:PSS aqueous dispersions are commercially available and used as a hole transport layer (HTL) in PSCs due to high hole affinity and high work function. The insertion of a thin PEDOT:PSS layer can raise the cohesion and/or change the work functions of the electrodes, and thus lower the interfacial series resistance.[31] However, PEDOT:PSS suffers from low conductivity, <1 S/cm, which is lower by one or two orders of magnitude than that of some other conducting polymers.[32] The conductivity of the PEDOT:PSS film must be increased for many applications. Therefore, for various applications, modification in the preparation of the PEDOT:PSS layer is mandatory. PSCs using this low conductivity PEDOT:PSS as the interface layer yield poor device performances. Hence, it is necessary to increase the conductivity of PEDOT:PSS for an effective HTL. It is highly possible to enhance its conductivity by adding various high-boiling-point polar solvents.[33]

Several methods have been applied to increase the conductivity of the PEDOT:PSS films, for example, solvent additives in the PEDOT:PSS solution or thermal postdeposition treatment of the PEDOT:PSS film.[33–37] PEDOT:PSS solution by mixing of organic molecules, such as dimethyl sulfoxide (DMSO), dimethylformamide (DMF), tetrahydrofuran (THF), ethylene glycol (EG), etc., was performed in order to improve the conductivity.[37,38] Treatment with certain salts, carboxylic acids, or inorganic acids have also significantly enhanced the conductivity of the PDEOT:PSS film.[39–41] Several models have been reported, such as conformational change of conductive PEDOT chains,[41,42] the bonds breaking between PEDOT and PSS and their phase segregation,[43] reduction of excess PSS layer for better connectivity between inter-PEDOT chains,[44] and PSS coils associated with large protons that weakens the electrostatic interaction, thus increasing the intramolecular conductivity in the PEDOT,[45] in order to understand the mechanism of conductivity enhancement in the PEDOT:PSS films.

In the present study, we report on the improvement of photovoltaic parameters of the BHJ PSCs by the incorporation of a thin layer of PEDOT:PSS mixed with fluoro compounds such as hexafluoroacetone trihydrate (HFA · $3H_2O$) and hexafluoroisopropanol (HFIPA) with various concentrations by spin coating technique. We studied the effect of HFA and HFIPA solvent additives in a PEDOT:PSS layer as an HTL. We obtained enhanced PEDOT:PSS films conductivities of about 1053 and 746 S/cm after treatment with 4 vol. % HFA and 6 vol. % HFIPA, respectively. The high performance of the HTL is attributed to preferential phase segregation of PEDOT:PSS with HFA · $3H_2O$ and HFIPA solvent mixture treatments. The improved performance of the PSC was dependent on the structure of organic solvents and the concentration of fluoro compounds in PEDOT:PSS solution. Using these optimized buffer layers, conjugated PSCs with a poly[[9-(1-octylnonyl)-9H-carbazole-2,7-diyl]-2,5-thiophenediyl-2,1,3-benzothia-diazole-4,7-diyl-2,5 thiophenediyl] polymer:[6,6]-phenyl-C71-butyric acid methyl esters (PCDTBT:$PC_{71}BM$) BHJ have been produced on indium-tin-oxide (ITO) coated glass substrate. PSC devices are exhibited with a maximum PCE of 4.10% and 3.98% for HFA4% and HFIPA6%, respectively, with enhanced current density-voltage ($J–V$) characteristics. The function of the HFA and HFIPA mixed PEDOT:PSS hole extraction layer will be discussed in the views of structural, optical transparency, and surface morphology.

## 2 Experimental Results

PEDOT:PSS (Clevios PH1000, H. C. Starck, Goslar, Germany), PCDTBT (1-Material, Quebec, Canada), and $PC_{71}BM$ (American Dye Source, Quebec, Canada) are used without further purification. PEDOT:PSS aqueous solution (Clevios PH1000) was used as a host polymer. The solvent additive treatment was performed by 2, 4, and 6 vol. % of HFA · $3H_2O$ and HFIPA were added into PEDOT:PSS as additives. The solution mixture was stirred vigorously for 5 h, after which it was filtered using a 0.25-$\mu$m filter. The filtered PEDOT:PSS was then deposited by spin coating at 5000 rpm for 30 s on glass and ITO coated substrates, which were precleaned with detergent, pure water, ethanol, and methanol in ultrasonication. Pristine and additive-mixed PEDOT:PSS films were annealed at 140°C for 20 min in vacuum in order to remove the water. The electrical conductivities and the thicknesses of the films were measured using Vander Pauw four-point probe method with a Keithley 2400 sourcemeter and a Dektak II surface profilometer, respectively. Optical transmittance spectra of the films were recorded using a Shimadzu UV-2450 spectrometer. Micro-Raman scattering measurements were performed in the backscattering geometry using a Renishaw in Via Raman spectrometer (532 nm). AFM images were recorded with Seiko Instruments SPA 400-SPI 4000 operating under ambient conditions in dynamic force mode. Solar cells were fabricated using an active layer of PCDTBT and $PC_{71}BM$ (having 1:1.4 wt.% %) in chlorobenzene by spin coating at 1000 rpm for 60 s. Then the film was dried at room temperature for 1 h and had a thickness around ~105 nm. Finally, a 100-nm-thick Al layer was thermally deposited in a high vacuum of $1.3 \times 10^{-4}$ Pa. The active area of each device was 0.3 $cm^2$. The current-voltage characteristics of the fabricated PSC devices were measured by employing an Advantest R-6441 A.C. source meter and a 100 mW solar simulator (Newport Oriel, California) with a filter having an air mass of 1.5 G (AM 1.5 G). The contact angle was analyzed with an Excimer Inc., (Kanagawa, Japan) contact angle meter. Figures 1(a)–1(c) show the molecular structure of PEDOT:PSS, HFA, and HFIPA, the energy level diagram of the active layer, PEDOT;PSS, ITO, and Al electrode and schematic diagram of fabricated PSC structure (ITO/PEDOT:PSS/PCDTBT:$PC_{71}BM$/Al).

## 3 Results and Discussion

The thickness and electrical conductivity ($\sigma$) of the pristine, HFA · $3H_2O$, and HFIPA treated PEDOT:PSS films are presented in Table 1. The pristine PEDOT:PSS film, with a thickness of around 52 nm, had a conductivity of 0.2 S/cm. On the other hand, the conductivity was significantly improved by three orders of magnitude after adding different concentrations of HFA · $3H_2O$ and HFIPA into PEDOT:PSS aqueous solution directly. From Table 1, we observed that the conductivity of the film depends on the concentration of fluoro compounds in the PEDOT:
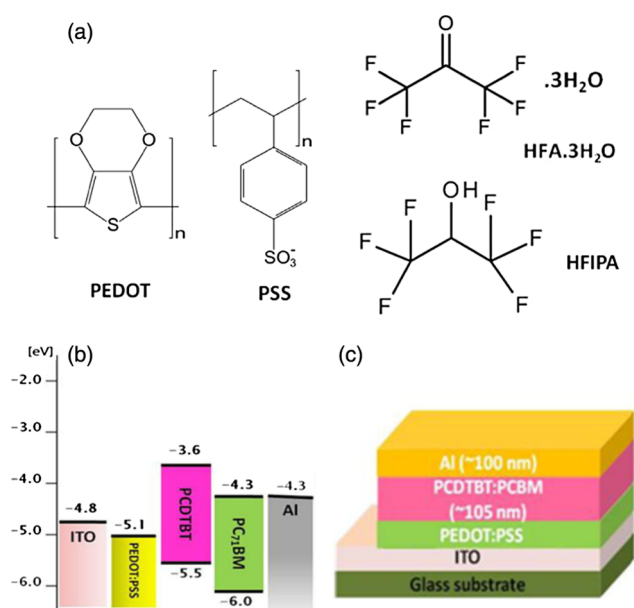
**Fig. 1.** (a) Molecular structures of PEDOT:PSS, PCDTBT, and PC$_{71}$BM. (b) Energy level diagram of the solar cell devices and (c) schematic device structure of the organic solar cell.

PSS film. Further, the high conductivity of 1053 S/cm was observed in 4 vol. % HFA treated PEDOT:PSS film which is nearly close to the conductivity of PEDOT:PSS film treated with HFA · 3H$_2$O (1164 S/cm) reported by Xia et al.[33] For HFIPA treated films, the high conductivity is only 746 S/cm obtained for 6 vol. % of HFIPA. Ouyang et al.[42] reported that PEDOT:PSS films conductivity enhancement is strongly dependent on the properties and structure of the organic compounds. The conductivity is negligible when organic solvent with only one –OH group is used, whereas significant conductivity enhancement can be observed for EG and other polyols, which has two –OH groups. The hydrolysis of HFA with water molecules results into hexafluoropropanal-2-2-diol (HFP2OH), a gem-diol with two –OH groups connected to one carbon atom. Moreover, HFP2OH is a highly amphiphilic compound with two hydrophobic CF$_3$ and two hydrophilic –OH groups. The hydrophobic nature of CF$_3$ can preferentially interact with hydrophobic PEDOT and the hydrophilic nature –OH groups preferentially interacts with the hydrophilic PSS. Consequently, some of the PEDOT chains are detached from the insulating PSS chain as a result of decrease in Coulombic attraction between PEDOT and PSS after HFA · 3H$_2$O treatment with various volume percentages.

Dimitriev et al. reported that the larger amount of protons associated with PSS chains equilibrate the negative charge on the PSS backbone and weaken its electrostatic interaction with the positively charged PEDOT. This leads to distortion of the planar PEDOT backbone and, therefore, to easier charge transfer along the PEDOT chain.[45] After the HFA · 3H$_2$O treatment, the PSS chains become PSSH chains by taking protons from other PSS chains, and PSSH phase segregation takes place. This further reduces the Coulombic attraction between the PEDOT and PSS chains and can give rise to conductivity enhancement.[46] For each HFA and HFIPA treated PEDOT:PSS film, we observed a reduction in film thickness (Table 1). The higher conductivity

**Table 1** Thickness and conductivity of PEDOT:PSS polymer films of pristine, HFA, and HFIPA treated.

| | 0% | | 2% | | 4% | | 6% | |
|---|---|---|---|---|---|---|---|---|
| Compound | Thickness (nm) | $\sigma$ (S/cm) | Thickness (nm) | $\sigma$ (S/cm) | Thickness (nm) | $\sigma$ (S/cm) | Thickness (nm) | $\sigma$ (S/cm) |
| HFA | 52 | 0.2 | 49 | 634 | 45 | 1053 | 44 | 971 |
| HFIPA | 52 | 0.2 | 52 | 399 | 50 | 518 | 48 | 746 |

of HFA-treated PEDOT:PSS film compared to that of HFIPA treatment can be attributed to the strong interaction between two –OH groups in the HFA · $3H_2O$ and the insulating PSSH-rich phase, whereas HFIPA has only one –OH group and we need further concentration of HFIPA in the film in order to increase the conductivity of the film.[47,48]

We measured the surface morphology of the polymer films by AFM, in order to confirm the effect of additives. Figures 2(a)–2(g) show the AFM images of PEDOT:PSS polymer film mixed with a different volume ratio of HFA and HFIPA additives. For comparison, height image of pristine PEDOT:PSS film is also presented in Fig. 2(a). Pristine PEDOT:PSS film reveals that the surface presents spherical type grain structures with dimensions of about 80 to 100 nm and a root-mean-square (rms) roughness of 1.01 nm. These grains are attributed to phase separated PEDOT:PSS domains surrounded by an excess of PSS chains.[47] The effect of HFA compound on PEDOT:PSS surface morphology can be clearly seen in Figs. 2(b)–2(d). The rms roughness for 2%, 4%, and 6% HFA treated polymer films was 1.22, 1.76, and 1.55 nm, respectively. After HFIPA treatment, the PEDOT:PSS films show different surface morphologies when compared with pristine PEDOT:PSS as shown in Figs. 2(e)–2(g). The rms roughness for 2%, 4%, and 6% HFIPA treated polymer films was 1.35, 1.41, and 1.73 nm, respectively. A remarkable difference in the AFM image can be observed for the 4% HFA and 6% HFIPA treated PEDOT:PSS film.

The surface features in the AFM image of HFA4% and HFIPA6% appear as entangled nanofibrous structures with dimensions of some tens of nanometers. This indicates the
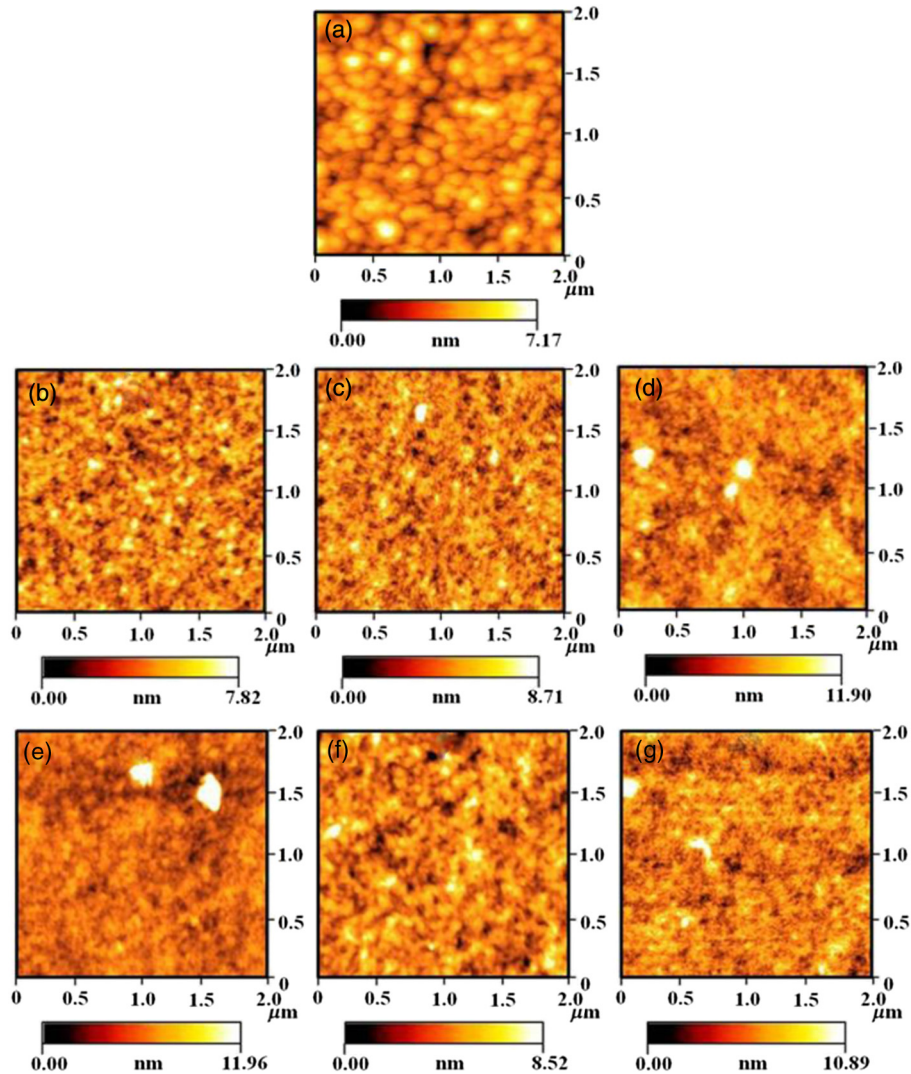


**Fig. 2.** Two-dimensional AFM images of PEDOT:PSS (a) pristine, (b) HFA2%, (c) HFA4%, (d) HFA6%, (e) HFIPA2%, (f) HFIPA4%, and (g) HFIPA6% thin films.

conformational change of polymer chains from coil to linear shape[49] after the HFA and HFIPA treatments, and these nanowires can promote charge transport more efficiently than spherical particles. In addition, the pristine PEDOT:PSS film had a roughness of 1.01 nm. The roughness was increased for PEDOT:PSS films treated with HFA and HFIPA compounds. The obtained roughness indicates that the interconnection channels between conductive PEDOT chains that spread out onto the planar substrate increased by the fluoro compounds treatment, thereby enhancing the conducting pathway.[50]

The optical transmittance spectra of HFA and HFIPA added PEDOT:PSS films on glass substrates were analyzed, as displayed in Figs. 3(a) and 3(b), respectively. The PEDOT:PSS films were quite smooth and had a uniform flat surface after the additive process. Transmittance is around 90% in the visible range for one-layer pristine PEDOT:PSS film, whereas a small reduction in transmittance was observed in 4 vol. % HFA addition. HFIPA treated films show a decrease in transmittance while pristine PEDOT:PSS films show relatively good transmittance, around 80% in the range from 400 to 900 nm. Due to the colorless nature of the PSS, the optical absorption in PEDOT:PSS mainly originates from the presence of PEDOT.

Figure 4 shows the Raman spectra of pristine and 4 vol. % HFA and 6 vol. % HFIPA treated PEDOT:PSS films. Clear differences between the Raman spectra of the pristine and the additive processed PEDOT:PSS films are evident in the range from 1400 to 1500 cm$^{-1}$. A shift in Raman peak position and change in band shape were observed in the C=C band of PEDOT:PSS after solvent additives.[51,52] Pristine PEDOT:PSS film exhibits a broad C=C symmetric stretching peak at 1445 cm$^{-1}$ with a shoulder part, whereas HFA4% and HFIPA6% treated films exhibit a narrower band and are shifted to the lower wave number of about 1436 cm$^{-1}$. The variations in the band stem from the changes in the electronic structure of PEDOT chains in PEDOT:PSS film upon additive treatment.[53] This change in Raman spectra is similar to that of EG treated PEDOT:PSS film observed by Ouyang et al.[42] They proposed that both coil and extended linear conformations present in a PEDOT:PSS film, and some of the coil conformations turn into linear conformation after EG solvent treatment. The benzoic structure may be favorable for a coil conformation and quinoid structure may be favorable for linear conformation. Therefore, the change in Raman spectra shape (Fig. 4) indicates that some PEDOT chains change from a benzoid to a quinoid structure. From the above analysis, the reduction of insulating PSS and the structural change of PEDOT in PEDOT:PSS films[54] upon mixing of HFA and HFIPA additives may enhance the conducting pathway in the PEDOT:PSS film.

To examine the effect of solvent-modified HTL layer on the device performance, the PSCs were fabricated with the structure of ITO/PEDOT:PSS/PCDTBT:PC$_{71}$BM/Al. The pristine and additive mixed PEDOT:PSS were chosen as a hole transport buffer layer. The PEDOT:PSS was sandwiched between the ITO and the PCDTBT:PC$_{71}$BM active layer. Figures 5(a) and 5(b) show the current density ($J$)–voltage ($V$) curves of the PSC devices with PEDOT:PSS layer that had been processed with HFA and HFIPA. Tables 2 and 3 list their photovoltaic parameters, such as open-circuit ($V_{oc}$), short-circuit current density ($J_{sc}$), fill factor (FF), and PCE. Figure 5(a)
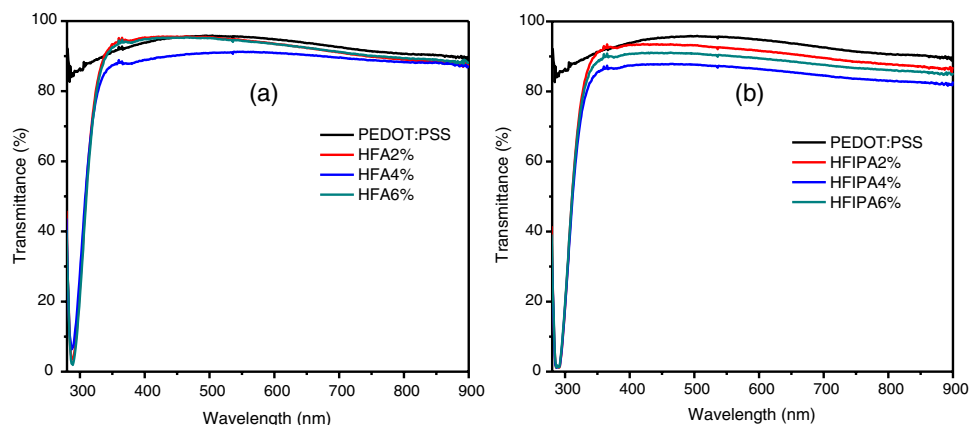


**Fig. 3.** UV–visible absorption spectra of the (a) HFA treated and (b) HFIPA treated PEDOT:PSS films on glass substrate.
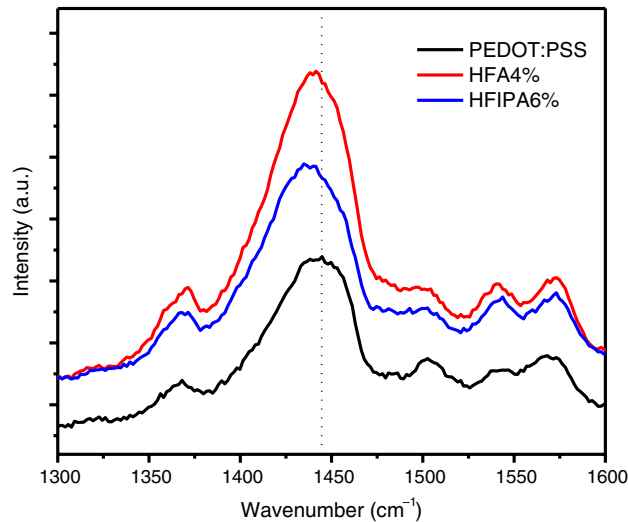
**Fig. 4.** Raman spectra of PEDOT:PSS films of pristine, HFA4%, and HFIPA6% on glass substrate.

shows the $J-V$ curves for devices incorporating PEDOT:PSS film treated with different concentrations of HFA. The $V_{oc}$ did not change much whereas $J_{sc}$ varied significantly after the additive process. The PCE increased from 2.72% for pristine to 3.36%, 4.10%, and 3.64% for 2, 4, and 6 vol. % of HFA treated PEDOT:PSS film, respectively. The series resistance ($R_s$) of the pristine, 2, 4, and 6 vol. % HFA treated PEDOT:PSS devices were 70.8, 55.2, 42.8, and 45.1 $\Omega$, respectively. Note the lower FF for pristine PEDOT:PSS device, indicating poor contact quality and leading to more recombination loss at the interface between the PEDOT:PSS and the PCDTBT:PC$_{71}$BM active layer. This clearly indicates that a 4 vol. % HFA treated PEDOT:PSS layer forms a good electrical contact between the ITO and the active layer of PCDTBT:PC$_{71}$BM.

Furthermore, we fabricated PSCs with HFIPA treated HTL and analyzed its impact on the device characteristics. From Fig. 5(b), the PSC devices that incorporated PEDOT:PSS film treated with HFIPA exhibit better device performance with increase of the concentration of HFIPA. The $J_{sc}$ of the device with 6 vol. % of HFIPA treated buffer layer exhibits higher than that of other devices along with a higher FF, leading to PCE of 3.98%. In the case of HFA treated films, the device shows performance increase up to 4 vol. % of HFA in the film and performance decrease for 6 vol. % of HFA. The $R_s$ of the devices for 2, 4, and 6 vol. % HFIPA treated PEDOT:PSS buffer layers was 56.3, 57.8 and 43.6 $\Omega$, respectively.
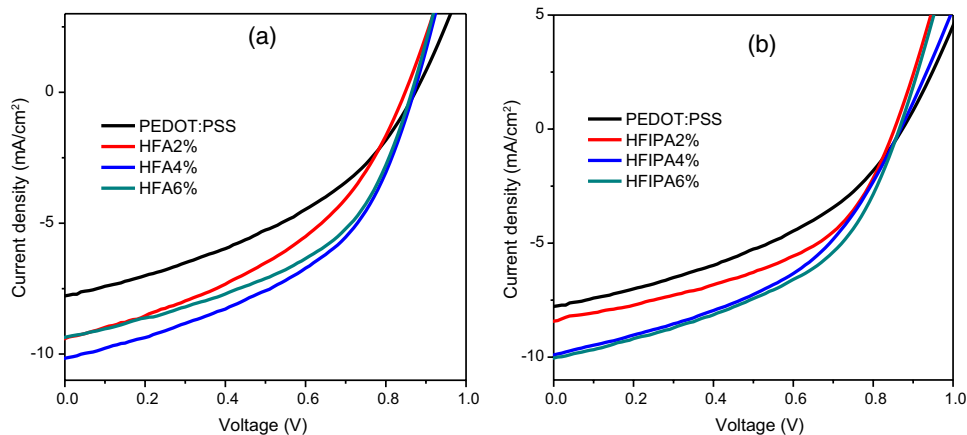


**Fig. 5.** The $J-V$ plots for PCDTBT:PC$_{71}$BM organic solar cells fabricated with (a) HFA and (b) HFIPA treated PEDOT:PSS as hole transport buffer layers under 100 mW/cm$^2$ illumination.

**Table 2** Photovoltaic parameters of PSC devices that incorporated pristine and HFA treated PEDOT:PSS as hole transport layer (HTL).

| PEDOT:PSS | $V_{oc}$ (V) | $J_{sc}$ (mA/cm$^2$) | Fill factor (FF) | PCE (%) | $R_s$ (Ω) |
|---|---|---|---|---|---|
| Pristine | 0.873 | 7.78 | 0.40 | 2.72 | 70.8 |
| HFA2% | 0.850 | 9.41 | 0.42 | 3.36 | 55.2 |
| HFA4% | 0.874 | 10.19 | 0.46 | 4.10 | 42.8 |
| HFA6% | 0.864 | 9.36 | 0.45 | 3.64 | 45.1 |

**Table 3** Photovoltaic parameters of PSC devices that incorporated pristine and HFIPA treated PEDOT:PSS as HTL.

| PEDOT:PSS | $V_{oc}$ (V) | $J_{sc}$ (mA/cm$^2$) | Fill factor (FF) | PCE (%) | $R_s$ (Ω) |
|---|---|---|---|---|---|
| Pristine | 0.873 | 7.78 | 0.40 | 2.72 | 70.8 |
| HFIPA2% | 0.853 | 8.42 | 0.43 | 3.09 | 56.3 |
| HFIPA4% | 0.868 | 9.90 | 0.44 | 3.78 | 57.8 |
| HFIPA6% | 0.864 | 10.03 | 0.46 | 3.98 | 43.6 |

Since the $J_{sc}$ and FF values dominantly influenced the PCE by the solvent additive process, the maximum PCE of 4.10% and 3.98% was obtained for 4 vol. % HFA and 6 vol. % HFIPA treated PEDOT:PSS. The observed trend is likely associated with the hole transport buffer layer characteristics, which depend on the structure and concentration of the fluoro compounds in the PEDOT:PSS layer. If the layer is without additive, the PSC would exhibit poor device efficiency because the hole transport characteristics between the ITO and the PCDTBT:PC$_{71}$BM active layer are poor. Moreover, poor adhesion between PEDOT:PSS HTL and the ITO substrate or with the PCDTBT:PC$_{71}$BM layer, often has resulted in devices with low efficiency.[55] In order to study the wettability of PEDOT:PSS on ITO substrate before and after HFA and HFIPA solvent treatments was analyzed from the static contact angle measurement. It is a simple, useful, and sensitive tool for quantifying the wetting property of different materials. Figures 6(a)–6(c) show the contact angle measurement of pure PEDOT:PSS and PEDOT:PSS treated with HFIPA and HFA solvents. The measurements were performed at 22°C and 48% relative humidity. We used PEDOT:PSS and solvent (HFA and HFIPA) treated PEDOT:PSS droplets to evaluate their adhesion to ITO substrate. The average contact angle for each sample was obtained by measuring four spots with PEDOT:PSS droplets with a volume of 10 $\mu$L. The standard error of contact angle measurements is ±1 deg. A droplet of PEDOT:PSS solution placed on ITO substrate shows a static contact angle of 27 deg [Fig. 6(a)]. The static contact angles measured for HFIPA and HFA solvents modified PEDOT:PSS solution on ITO substrate were 23 and 12 deg, respectively. This clearly indicates that the simple solvent mixing into PEDOT:PSS greatly improved the wetting effect between ITO and PEDOT:PSS treated with HFA. It is expected that the improved adhesion property of PEDOT:PSS with 6% HFA can decrease resistance at the interface and help better to transport holes from the active layer to ITO electrode. The increment in FF accompanied with the
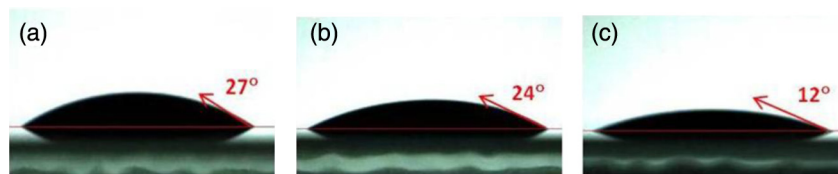


**Fig. 6.** Static contact angle photographs of the droplet (10 $\mu$L) of (a) PEDOT:PSS, (b) PEDOT:PSS with 6% HFIPA, and (c) PEDOT:PSS with 4% HFA on ITO substrate.

reduction in series resistance can be attributed to enhanced conductivity and the good adherence property of PEDOT:PSS with HFA and HFIPA treatments. The uniform film with close packing of fine nanofibrous structures improves the transport of charge carriers and decreases the series resistance due to better contacts.

## 4 Conclusion

We have investigated the surface, optical, and structural modifications of PEDOT:PSS films based on fluoro compound additive processes with various concentrations. The electrical conductivity of as-prepared PEDOT:PSS films can be significantly enhanced by the addition of HFA and HFIPA and the film transmittance is over 80%, compared to the commercial ITO substrate. The enhancement of the conductivity is attributed to preferential phase segregation of PSS chain induced by the HFA and HFIPA as well as a conformational change of the PEDOT chains in the PEDOT:PSS polymer films. AFM images showed the presence of entangled nanofibrous structures which enhance the conducting pathway. Thin layers of PEDOT:PSS treated with HFA and HFIPA as HTL provide an explanation for the interesting device characteristics of the PSC. The additive process has allowed the lowering of the series resistance of the obtained devices and this indicates that an optimized hole buffer layer can improve the device performance of OSCs. The PCE of the device with pristine PEDOT:PSS buffer layer was 2.72% together with low $J_{sc}$ and FF. We obtained a high PCE of 4.10% and 3.98% in the PSC with a 4 vol. % HFA and 6 vol. % HFIPA treated PEDOT:PSS layer, respectively.

## Acknowledgments

## References

1. J. E. Slota, X. He, and W. T. S. Huck, "Controlling nanoscale morphology in polymer photovoltaic devices," *Nano Today* **5**(3), 231–242 (2010), http://dx.doi.org/10.1016/j.nantod.2010.05.004.
2. M. Jorgensen et al., "Stability of polymer solar cells," *Adv. Mater.* **24**(5), 580–612 (2012), http://dx.doi.org/10.1002/adma.201104187.
3. Y. Liang and L. Yu, "A new class of semiconducting polymers for bulk heterojunction solar cells with exceptionally high performance," *Acc. Chem. Res.* **43**(9), 1227–3126 (2010), http://dx.doi.org/10.1021/ar1000296.
4. S. Gunes, H. Neugebauer, and N. S. Sariciftci, "Conjugated polymer-based organic solar cells," *Chem. Rev.* **107**(4), 1324–1338 (2007), http://dx.doi.org/10.1021/cr050149z.
5. Y. T. Tsai et al., "Charge transporting properties and output characteristics in polythiophene: fullerene derivative solar cells," *Jpn. J. Appl. Phys.* **50**, 01BC13 (4 pages) (2011), http://dx.doi.org/10.7567/JJAP.50.01BC13.
6. L. Saitoh et al., "Performance of spray deposited poly [N-9''-hepta-decanyl-2,7- carbazole-alt-5,5-(4',7'-di-2-thienyl-2',1',3'-benzothiadiazole)]/[6,6]-phenyl-C61-butyric acid methyl ester blend active layer based bulk heterojunction organic solar cell devices," *Thin Solid Films* **520**(7), 3111–3117 (2012), http://dx.doi.org/10.1016/j.tsf.2011.12.022.
7. C. J. Brabec et al., "Polymer-fullerene bulk-heterojunction solar cells," *Adv. Mater.* **22**, 3839–3856 (2010), http://dx.doi.org/10.1002/adma.200903697.
8. J. Peet et al., "Efficiency enhancement in low-bandgap polymer solar cells by processing with alkane dithiols," *Nat. Mater.* **6**(7), 497–500 (2007), http://dx.doi.org/10.1038/nmat1928.
9. S. H. Park et al., "Bulk heterojunction solar cells with internal quantum efficiency approaching 100%," *Nat. Photonics* **3**, 297–302 (2009), http://dx.doi.org/10.1038/nphoton.2009.69.

10. Z. He et al., "Simultaneous enhancement of open-circuit voltage, short-circuit current density, and fill factor in polymer solar cells," *Adv. Mater.* **23**(40), 4636–4643 (2011), http://dx.doi.org/10.1002/adma.201103006.

11. Z. He et al., "Enhanced power-conversion efficiency in polymer solar cells using an inverted device structure," *Nat. Photonics* **6**, 591–595 (2012), http:/dx.doi.org/10.1038/nphoton.2012.190.

12. B. Carsten et al., "Examining the effect of the dipole moment on charge separation in donor-acceptor polymers for organic photovoltaic applications," *J. Am. Chem. Soc.* **133**(50), 20468–20475 (2011), http://dx.doi.org/10.1021/ja208642b.

13. B. C. Thompson and J. M. Frechet, "Polymer-fullerene composite solar cells," *Angew. Chem. Int. Ed. Engl.* **47**(1), 58–77 (2008), http://dx.doi.org/10.1002/(ISSN)1521-3773.

14. H. J. Son et al., "Overcoming efficiency challenges in organic solar cells: rational development of conjugated polymers," *Energy Environ. Sci.* **5**(8), 8158–8170 (2012), http://dx.doi.org/10.1039/c2ee21608f.

15. S. Kannappan et al., "Fabrication and characterizations of PCDTBT: PC71BM bulk heterojunction solar cell using air brush coating method," *J. Mater. Sci.* **48**(6), 2308–2317 (2013), http://dx.doi.org/10.1007/s10853-012-7010-1.

16. S. Wakim et al., "Charge transport, photovoltaic, and thermoelectric properties of poly (2,7–carbazole) and poly(indolo[3,2–b]carbazole) derivatives," *Polym. Rev.* **48**(3), 432–462 (2008), http://dx.doi.org/10.1080/15583720802231726.

17. S.-P. Yang et al., "Highly efficient PCDTBT:PC71 BM based photovoltaic devices without thermal annealing treatment," *Chin. Phys. Lett.* **28**(12), 128401 (4 pages) (2011), http://dx.doi.org/10.1088/0256-307X/28/12/128401.

18. T.-Y. Chu et al., "Morphology control in polycarbazole based bulk heterojunction solar cells and its impact on device performance," *Appl. Phys. Lett.* **98**(25), 253301 (3 pages) (2011), http://dx.doi.org/10.1063/1.3601474.

19. D. H. Wang et al., "Enhanced power conversion efficiency in PCDTBT/PC70BM bulk heterojunction photovoltaic devices with embedded silver nanoparticle clusters," *Adv. Energy Mater.* **1**(5), 766–770 (2011), http://dx.doi.org/10.1002/aenm.v1.5.

20. A. Benor et al., "Efficiency improvement of fluorescent OLEDs by tuning the working function of PEDOT:PSS using UV–ozone exposure," *Org. Electron.* **11**(5), 938–945 (2010), http://dx.doi.org/10.1016/j.orgel.2010.02.014.

21. S. K. M. Jönsson et al., "Photoelectron spectroscopy of the contact between the cathode and the active layers in plastic solar cells: the role of LiF," *Jpn. J. Appl. Phys.* **44**(6A), 3695–3701 (2005), http://dx.doi.org/10.1143/JJAP.44.3695.

22. F. Cheng et al., "Enhancing the performance of P3HT:ICBA based polymer solar cells using LiF as electron collecting buffer layer and UV–ozone treated MoO3 as hole collecting buffer layer," *Sol. Energy Mater. Sol. Cells* **110**, 63–68 (2013), http://dx.doi.org/10.1016/j.solmat.2012.12.006.

23. F. Zhang et al., "Effect of an ultra-thin molybdenum trioxide layer and illumination intensity on the performance of organic photovoltaic devices," *Energy Fuels* **24**(7), 3739–3742 (2010), http://dx.doi.org/10.1021/ef901325e.

24. J.-S. Huang et al., "Efficient and air-stable polymer photovoltaic devices with wo3–v2o5 mixed oxides as anodic modification," *IEEE Electron. Device Lett.* **31**(4), 332–334 (2010), http://dx.doi.org/10.1109/LED.2009.2039846.

25. K. X. Steirer et al., "Solution deposited NiO thin-films as hole transport layers in organic photovoltaics," *Org. Electron.* **11**(8), 1414–1418 (2010), http://dx.doi.org/10.1016/j.orgel.2010.05.008.

26. C. Tao et al., "Role of tungsten oxide in inverted polymer solar cells," *Appl. Phys. Lett.* **94**(4), 43311 (3 pages) (2009), http://dx.doi.org/10.1063/1.3076134.

27. C. Waldauf et al., "Highly efficient inverted organic photovoltaics using solution based titanium oxide as electron selective contact," *Appl. Phys. Lett.* **89**(23), 233517 (3 pages) (2006), http://dx.doi.org/10.1063/1.2402890.

28. E. Ahlswede, J. Hanisch, and M. Powalla, "Comparative study of the influence of LiF, NaF, and KF on the performance of polymer bulk heterojunction solar cells," *Appl. Phys. Lett.* **90**(16), 163504 (3 pages) (2007), http://dx.doi.org/10.1063/1.2723077.

29. F.-C. Chen, "Cesium carbonate as a functional interlayer for polymer photovoltaic devices," *J. Appl. Phys.* **103**(10), 103721 (5 pages) (2008), http://dx.doi.org/10.1063/1.2937202.

30. T. Stubhan et al., "Inverted organic solar cells using a solution processed aluminum-doped zinc oxide buffer layer," *Org. Electron.* **12**(9), 1539–1543 (2011), http://dx.doi.org/10.1016/j.orgel.2011.05.027.

31. S. H. Lee et al., "Effect of interface thickness on power conversion efficiency of polymer photovoltaic cells," *Electron. Mater. Lett.* **5**(1), 47–50 (2009), http://dx.doi.org/10.3365/eml.2009.03.047.

32. J. Ouyang et al., "Polymer optoelectronic devices with high-conductivity poly(3,4-ethylenedioxythiophene) anodes," *J. Macromol. Sci.* **41**(12), 1497–1511 (2004), http://dx.doi.org/10.1081/MA-200035426.

33. Y. Xia, K. Sun, and J. Ouyang, "Highly conductive poly(3,4-ethylenedioxythiophene):poly(styrene sulfonate) films treated with an amphiphilic fluoro compound as the transparent electrode of polymer solar cells," *Energy Environ. Sci.* **5**(1), 5325 (2012), http://dx.doi.org/10.1039/c1ee02475b.

34. W. Cai, X. Gong, and Y. Cao, "Polymer solar cells: recent development and possible routes for improvement in the performance," *Sol. Energy Mater. Sol. Cells* **94**(2), 114–127 (2010), http://dx.doi.org/10.1016/j.solmat.2009.10.005.

35. Y. Xia and J. Ouyang, "PEDOT:PSS films with significantly enhanced conductivities induced by preferential solvation with cosolvents and their application in polymer photovoltaic cells," *J. Mater. Chem.* **21**, 4927–4936 (2011), http://dx.doi.org/10.1039/c0jm04177g.

36. P. A. Levermore et al., "Fabrication of highly conductive poly(3,4-ethylenedioxythiophene) films by vapor phase polymerization and their application in efficient organic light-emitting diodes," *Adv. Mater.* **19**(17), 2379–2385 (2007), http://dx.doi.org/10.1002/(ISSN)1521-4095.

37. Y. H. Kim et al., "Highly conductive PEDOT:PSS electrode with optimized solvent and thermal post-treatment for ITO-free organic solar cells," *Adv. Func. Mater.* **21**(6), 1076–1081 (2011), http://dx.doi.org/10.1002/adfm.201002290.

38. J. Y. Kim et al., "Enhancement of electrical conductivity of poly(3,4-ethylenedioxythiophene)/poly(4-styrenesulfonate) by a change of solvents," *Synth. Met.* **126**(2–3), 311–316 (2002), http://dx.doi.org/10.1016/S0379-6779(01)00576-8.

39. Y. Xia and J. Ouyang, "Significant conductivity enhancement of conductive poly(3,4-ethylenedioxythiophene):poly(styrenesulfonate) films through a treatment with organic carboxylic acids and inorganic acids," *ACS Appl. Mater. Interfaces* **2**(2), 474–483 (2010), http://dx.doi.org/10.1021/am900708x.

40. Y. Xia and J. Ouyang, "Anion effect on salt-induced conductivity enhancement of poly(3,4-ethylenedioxythiophene):poly(4-styrenesulfonate) films," *Org. Electron.* **11**(6), 1129–1135 (2010), http://dx.doi.org/10.1016/j.orgel.2010.04.007.

41. H. Y. Xia and J. Ouyang, "Salt-induced charge screening and significant conductivity enhancement of conducting poly(3,4-ethylenedioxythiophene):poly(styrenesulfonate)," *Macromolecules* **42**(12), 4141–4147 (2009), http://dx.doi.org/10.1021/ma900327d.

42. J. Ouyang et al., "On the mechanism of conductivity enhancement in poly(3,4-ethylenedioxythiophene):poly(styrene sulfonate) film through solvent treatment," *Polymer* **45**(25), 8443–8450 (2004), http://dx.doi.org/10.1016/j.polymer.2004.10.001.

43. B. J. de Gans, P. C. Duineveld, and U. S. Schubert, "Inkjet printing of polymers: state of the art and future developments," *Adv. Mater.* **16**(3), 203–213 (2004), http://dx.doi.org/10.1002/(ISSN)1521-4095.

44. S. K. M. Jönsson et al., "The effects of solvents on the morphology and sheet resistance in poly(3,4-ethylenedioxythiophene)–polystyrenesulfonic acid (PEDOT-PSS) films," *Synth. Met.* **139**(1), 1–10 (2003), http://dx.doi.org/10.1016/S0379-6779(02)01259-6.

45. O. P. Dimitriev, Y. P. Piryatinski, and A. A. Pud, "Evidence of the controlled interaction between PEDOT and PSS in the PEDOT:PSS complex via concentration changes of the complex solution," *J. Phys. Chem. B* **115**(6), 1357–1362 (2011), http://dx.doi.org/10.1021/jp110545t.

46. N. A. D. Yamamoto et al., "Modification of PEDOT:PSS anode buffer layer with HFA for flexible polymer solar cells," *Chem. Phys. Lett.* **572**, 73–77 (2013), http://dx.doi.org/10.1016/j.cplett.2013.04.022.

47. U. Lang et al., "Microscopical investigations of PEDOT:PSS thin films," *Adv. Funct. Mater.* **19**(8), 1215–1220 (2009), http://dx.doi.org/10.1002/adfm.v19:8.

48. Y. Xia and J. Ouyang, "Highly conductive PEDOT:PSS films prepared through a treatment with geminal diols or amphiphilic fluoro compounds," *Org. Electron.* **13**(10), 1785–1792 (2012), http://dx.doi.org/10.1016/j.orgel.2012.05.039.

49. M. Reyes-Reyes, I. Cruz-Cruz, and R. López-Sandoval, "Enhancement of the electrical conductivity in PEDOT:PSS films by the addition of dimethyl sulfate," *J. Phys. Chem. C* **114**(47), 20220–20224 (2010), http://dx.doi.org/10.1021/jp107386x.

50. X. Crispin et al., "The origin of the high conductivity of poly(3,4-ethylenedioxythiophene)-poly(styrenesulfonate) (PEDOT-PSS) plastic electrodes," *Chem. Mater.* **18**(18), 4354–4360 (2006), http://dx.doi.org/10.1021/cm061032+.

51. M. Lapkowski and A. Pron, "Electrochemical oxidation of poly(3,4-ethylenedioxythiophene)—'in situ' conductivity and spectroscopic investigations," *Synth. Met.* **110**(1), 79–83 (2000), http://dx.doi.org/10.1016/S0379-6779(99)00271-4.

52. S. Garreau, J. L. Duvail, and G. Louarn, "Spectroelectrochemical studies of poly(3,4-ethylenedioxythiophene) in aqueous medium," *Synth. Met.* **125**(3), 325–329 (2001), http://dx.doi.org/10.1016/S0379-6779(01)00397-6.

53. Y. Xia, H. Zhang, and J. Ouyang, "Highly conductive PEDOT:PSS films prepared through a treatment with zwitterions and their application in polymer photovoltaic cells," *J. Mater. Chem.* **20**, 9740–9747 (2010), http://dx.doi.org/10.1039/c0jm01593h.

54. Y. Xia and J. Ouyang, "Significant different conductivities of the two grades of poly(3,4-ethylenedioxythiophene):poly(styrenesulfonate), Clevios P and Clevios Ph1000, arising from different molecular weights," *ACS Appl. Mater. Interfaces* **4**(8), 413–41401 (2012), http://dx.doi.org/10.1021/am300881m.

55. L. Chen et al., "Efficient bulk heterojunction polymer solar cells using PEDOT/PSS doped with solution-processed MoO as anode buffer layer," *Sol. Energy Mater. Sol. Cells* **102**, 66–70 (2012), http://dx.doi.org/10.1016/j.solmat.2012.03.027.

Biographies of the authors are not available.